

Constrained Coding for Quasi-Linear Optical Data Transmission Systems

Vladimir Pechenkin and Frank R. Kschischang, *Fellow, IEEE*

Abstract—This paper considers the application of constrained coding to 40-Gb/s dispersion-managed single-channel optical communication systems limited by intrachannel four-wave mixing (IFWM). It is shown that when transmitted sequences obey the so-called $(2, \infty)$ constraint, runlength-limited codes can be designed to not only suppress ghost pulse formation but also improve the data rate by as much as 50% without increasing the transmission bandwidth. Since IFWM is a highly pattern-dependent effect, coding schemes with certain characteristics are preferable. Two different codes with simple encoding and decoding algorithms are constructed, and their performance is analyzed and compared to that of a realistic benchmark system. One of the codes turns out to be consistently better than the other due to its superior statistical properties. The qualitative conclusions are confirmed by numerical simulations. An extension of the method to multichannel links is also considered, and similar gain in data rate is demonstrated.

Index Terms—Constrained coding, fiber-optic communications, ghost pulses, intrachannel four-wave mixing (IFWM).

I. INTRODUCTION

FIBER nonlinearity is known to be a major performance-limiting factor in long-haul dispersion-managed fiber-optic communication systems operating at bit rates of 40 Gb/s per channel or higher. A popular approach to mitigating this channel impairment is the so-called quasi-linear (or pseudolinear) regime of transmission [1]–[6]. After being launched into the fiber, optical pulses quickly disperse and spread over tens, hundreds, or even thousands of bit slots. Then, with the help of dispersion compensation, individual pulses can be compressed back to their initial shape, and the original waveform can be reproduced with only a slight degradation. The key idea is to make the intensity pattern change so rapidly that the effect of fiber nonlinearity averages out [1].

It is widely recognized that quasi-linear systems, even multichannel ones, are mostly limited by intrachannel nonlinear impairments. In particular, intrachannel four-wave mixing (IFWM) results in the energy transfer between marks and the creation of ghost (or shadow) pulses in spaces. Return-to-zero pulses used for the transmission of “1”s also experience timing jitter caused by intrachannel cross-phase modulation (IXPM).

While IXPM is usually reduced by clever dispersion management [3], [7], the suppression of IFWM is not so clear cut. A number of different techniques have been proposed,

including phase coding [8], [9], unequally spaced pulses [10], alternating polarizations [11], optical phase conjugation [12], and constrained coding [13]–[17].

The last approach is the focus of this paper, although our idea is quite different. IFWM can be considered as a form of intersymbol interference, and its impact strongly depends on the minimum pulse separation Δ . In fact, the intensity of the IFWM-induced perturbation is known to scale in proportion to $E_0^3 \tau_0 / \Delta^4$ [1], where E_0 is the pulse energy, and τ_0 is its width. If Δ coincides with the bit slot duration T_B (as is usually the case in practice), IFWM-related problems grow as T_B^{-4} as well.

In [13]–[16], various constraints are imposed on transmitted sequences in order to avoid bit patterns that lead to the formation of the strongest ghost pulses. The symbol rate, however, remains the same, causing a significant decrease in the data rate of the constrained system, compared with the benchmark system. Consequently, in order to make a fair comparison between the two, the symbol rate must be increased, i.e., both T_B and Δ have to be reduced. The shrinking of Δ , however, enhances nonlinear pulse interactions according to the Δ^{-4} law and diminishes the gain from constrained coding. For example, the rates of the codes proposed in [15] lie in the range of 0.76–0.83. Hence, the IFWM strength in a 40-Gb/s link employing one of those schemes is expected to be greater by a factor of 2.1–3. The code introduced in [16] has a rate of only 2/3, which implies an IFWM enhancement by a factor of 5 in a constrained system of the same data rate. Such a comparison with a benchmark system of equal capacity is essential but has not been done in the previous work.

In this paper, we show that an accurately designed constrained code not only mitigates ghost pulses but also provides a data rate improvement of up to 50%! Our idea of IFWM reduction for the whole system is based on the following argument. Unlike previous work, we do not equate T_B with Δ . When constraints are introduced, T_B has to be shrunk to maintain the same data rate. However, it does not mean that Δ must also be reduced. On the contrary, Δ may be even greater than that for the benchmark system. In this case, the Δ^{-4} law is expected to work in our favor and suppress IFWM-induced perturbations.

The gain in data rate comes from the following observation: Since shorter pulses are less affected by IFWM, a low duty cycle is preferable. Certainly, systems designed in such a way may have much “white space” between “1”s and are less attractive from the spectral efficiency point of view. We will show how the application of constrained coding can turn this seemingly redundant white space into extra information. A conclusion

Manuscript received May 11, 2006; revised August 29, 2006.

The authors are with The Edward S. Rogers Sr. Department of Electrical and Computer Engineering, University of Toronto, Toronto, ON M5S 3G4, Canada (e-mail: vlad@comm.utoronto.ca; frank@comm.utoronto.ca).

Digital Object Identifier 10.1109/JLT.2006.884973

that the introduction of constraints can actually increase the data rate looks very surprising. However, this approach is one of the cornerstones of magnetic and optical recording systems [18].

The remainder of this paper is organized as follows: In Section II, we design a single-channel benchmark system and discuss various related aspects. Section III presents constrained codes based on the so-called $(2, \infty)$ runlength-limited (RLL) constraint and explains why they can be beneficial. Section IV contains the major results of this paper. The codes constructed in Section III are applied to the benchmark system developed in Section II. We analyze their performance and show that the choice of a coding scheme is important. In all cases, a data rate improvement of about 50% is demonstrated. Section V is devoted to multichannel experiments, where we show that the constrained coding approach can be successfully extended to wavelength-division-multiplexed (WDM) links as well. Section VI discusses other important issues relevant to our study.

II. BENCHMARK SYSTEM DESIGN

In this paper, we consider long-haul optically amplified ON-OFF-keyed systems operating in the quasi-linear regime. We assume that the bit rate B is high enough to make IFWM a paramount concern. We also take into account IXPM and Gordon-Haus timing jitter. At the same time, B must be low enough so that effects like Raman-induced timing jitter can safely be neglected. We do not include the influence of third-order dispersion or polarization-mode dispersion either.

When optical amplifiers are inserted periodically to compensate for fiber losses, amplified spontaneous emission (ASE) noise generated by the amplifiers accumulates over the entire link and ultimately degrades the optical signal-to-noise ratio (OSNR). Therefore, a certain minimum pulse energy E_0 is required to provide a satisfactory OSNR at the receiver. On the other hand, the intensity of IFWM-induced perturbations is proportional to E_0^3 if the pulse width τ_0 is fixed [1]. The key design tradeoff is to select the value of E_0 in such a way that the contributions from ASE and IFWM to the probability of error p_u at the receiver are somehow balanced. Here, the index “u” stands for “unconstrained.”

A 40-Gb/s “benchmark” system ($T_B = 25$ ps) is designed as follows: The dispersion map consists of a 40-km-long segment of a standard fiber with $D_+ = 17$ ps/(nm · km) followed by a reverse dispersion fiber of the same length and exactly opposite dispersion $D_- = -17$ ps/(nm · km). To reduce the IXPM-induced timing jitter, we use a precompensating fiber of length 17.5 km and dispersion D_- along with a postcompensating fiber of the same length and dispersion D_+ . The average dispersion of the link is thus zero. All fibers have an attenuation of 0.25 dB/km and a nonlinear parameter of 2.5 W⁻¹/km. Optical amplifiers are placed every 80 km at the beginning of the anomalous dispersion span, their spontaneous emission factor being 1.4. The transmission distance is 4835 km including the compensating sections. The dispersion profile of the link is sketched in Fig. 1, where the amplifiers are represented by triangles.

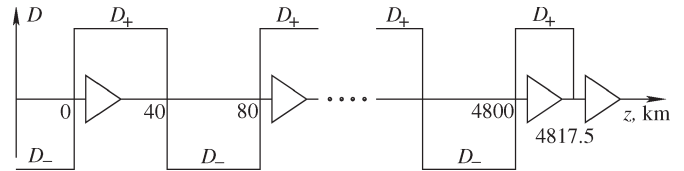


Fig. 1. Dispersion profile of the link.

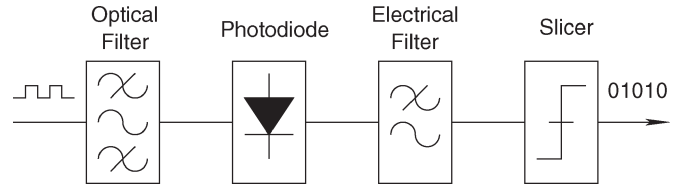


Fig. 2. Receiver structure.

Gaussian pulses of width $\tau_0 = 3$ ps, peak power P_0 , and energy $E_0 = \sqrt{\pi} P_0 \tau_0$ are transmitted. Their envelope $A(t)$ may be written as

$$A(t) = \sqrt{P_0} \exp\left(-\frac{t^2}{2\tau_0^2}\right). \quad (1)$$

The standard deviation of the overall timing jitter is found to always be below 1.2 ps, which implies its negligible contribution to p_u .

The receiver has a simple structure and consists of an ideal optical bandpass filter, a photodiode, an integrate-and-dump electrical filter, and a slicer (Fig. 2). The photodiode is modeled as a square-law detector with quantum efficiency $\eta = 0.9$. In the linear regime of operation, where ASE-induced amplitude jitter dominates, p_u can be computed as in [19] and [20]. The bandwidth of the optical filter is chosen to be $B_o = 280$ GHz for two reasons. First, the pulse shape remains almost the same after filtering. Second, the number of noise modes $2B_o T_B$ becomes an even integer, which considerably simplifies the calculation of p_u .

To make a stringent test of our coding schemes, the benchmark system is allowed to have p_u as large as 10^{-2} . We assume that an error-correcting code (ECC) may be applied afterward to achieve the target bit error rate. This setup also makes it feasible to estimate the bit error rate and the corresponding channel capacity C_u by directly counting the number of errors observed at the receiver. The details of how C_u is calculated are provided in Section III-C.

Numerical simulations were carried out for 8192-bit de Bruijn pseudorandom input sequences using the split-step Fourier method with flexible step size [21]. Such a large number of transmitted bits is essential for an accurate representation of intrachannel nonlinear effects [22]. We varied P_0 in the range of 4–12 mW to find the best operating point. Equivalently, E_0 ranged from 21.3 to 63.8 fJ. When $P_0 < 4$ mW, the influence of IFWM is negligible, and p_u was in a good agreement with [20]. For example, $p_u = 0.018$ when $P_0 = 4$ mW. However, the optimum P_0 was found to be around 6–8 mW (the lower curve in Fig. 3). The minimum p_u was about 0.007, which corresponds to the channel capacity of approximately 37.5 Gb/s. In this region of operation, ghost pulses make a significant

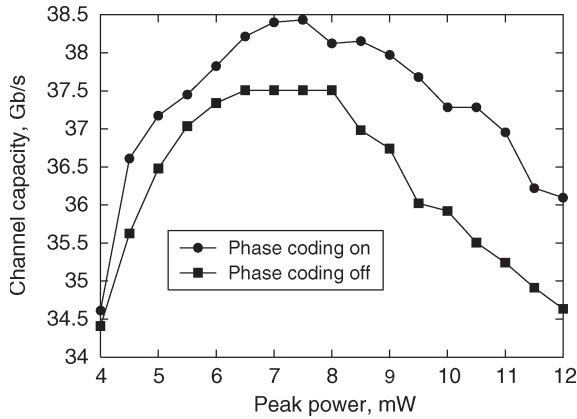


Fig. 3. Benchmark system capacity with and without phase coding.

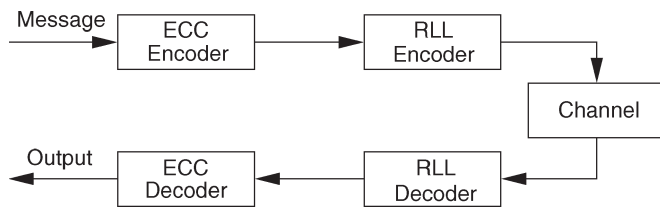


Fig. 4. Traditional ECC-RLL concatenation.

contribution to the probability of error (which would be 0.002 or less in a purely linear regime).

We also simulated a benchmark system with additional phase coding [8] by introducing a phase shift of π for every other pulse. This type of line coding (alternate mark inversion) suppresses the strongest ghosts by virtue of destructive interference and often improves the system performance. Indeed, our simulations confirmed that the channel capacity is somewhat higher in this case, reaching a peak value of about 38.4 Gb/s. Still, IFWM eventually overwhelms the system (the upper curve in Fig. 3).

III. RLL CODING SCHEMES

A. Coding for Constrained Channels

A binary channel is said to be RLL or (d, k) constrained if channel sequences are required to have at least d but at most k “0”s between any pair of adjacent “1”s. Information transmission through an RLL channel implies two necessary steps. First, an arbitrary source word must be mapped unambiguously to a sequence that satisfies the channel constraints. Second, some error control must be implemented to protect the data from noise. A popular approach is to utilize a concatenation of an inner modulation RLL (or constrained) code with an outer ECC (Fig. 4). A message to be transmitted is first encoded with the ECC. The result is supplied to the RLL encoder (or modulator). The modulator transforms an incoming unconstrained word to a channel sequence that satisfies the required constraints. At the receiver, the decoders work in the reverse order. The received word is first demodulated by the RLL decoder (or demodulator), and the ECC decoder cleans up possible errors afterward.

Proper design of the ECC requires knowledge of the intermediate channel at the output of the demodulator. Knowledge

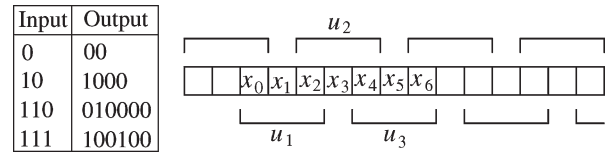


Fig. 5. Encoding table and decoding algorithm for RLL code C_1 .

of the physical channel is insufficient as errors may also be introduced by the RLL decoder itself. This phenomenon is referred to as error propagation or error amplification and may considerably increase the burden on the ECC. In principle, if a reasonable information-theoretic model of the physical link can be constructed, the intermediate channel may be estimated quite accurately [23], [24]. The combined effect of ASE and IFWM, however, is not so easily translated into the language of information theory. Therefore, in this paper, the channel statistics are obtained from Monte Carlo simulations.

B. RLL Code Construction

In this paper, we impose the $(2, \infty)$ constraint on transmitted sequences, i.e., a mark is always followed by two or more spaces. The theory of constrained coding is well developed [18], and it is known that the capacity of a $(2, \infty)$ -constrained system is approximately 0.5515 [18, Table V-C]. Hence, it should be possible to design a rate 1/2 coding scheme with simple and fast encoding and decoding algorithms keeping the rate efficiency high enough at the same time.

Many codes with different properties can be constructed. It is clear that a good scheme must reduce error propagation as much as possible, while other desirable characteristics are less obvious. In Section IV, we will compare the performance of two different RLL codes with extremely limited error amplification and discuss some of their important features.

The first code C_1 was originally proposed in [23] and [24]. The modulator works as follows: First, a source word $u = (u_1, \dots, u_m)$ of length m is parsed into elementary blocks of at most 3 bits, only the blocks from the first column of the encoding table in Fig. 5 being allowed. If u has “01” or “011” at the end, a dummy “0” is appended to u . Each block is then mapped to the corresponding channel sequence. The final result is a codeword x of length $n = 2m$ (or $2m + 2$). If an extra “0” was appended to u , the two trailing “0”s of x are discarded. For example, let $u = “101.”$ After a dummy “0” is appended, u parses as “10,” “10.” Since “10” maps to “1000,” $x = “10001000.”$ We discard the last two “0”s and finally obtain $x = “100010.”$

To concatenate two constrained words $x = (x_1, \dots, x_n)$ and $y = (y_1, \dots, y_n)$ without a constraint violation, a trick from [25] may be employed. Note that x_n is always 0. The two constraints can then be violated if and only if $x_{n-1} = y_1 = 1$. In this case, we set $x_{n-1} = y_1 = 0$ and $x_n = 1$. Thus, x_n works as a merging bit, which must be used for the decoding of both x and y .

The demodulator is implemented in a sliding-window fashion (Fig. 5). A window of length three slides along the word $x = (x_0, x_1, \dots, x_n)$ by two positions each time. Here, x_0

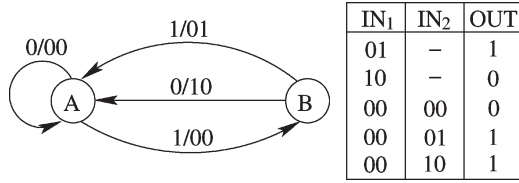


Fig. 6. Encoding machine and decoding table for RLL code C_2 .

symbolically denotes the last (merging) bit of the preceding codeword. The i th output bit is the logical “OR” of all 3 bits in the window, i.e., $u_i = x_{2i-2} + x_{2i-1} + x_{2i}$, $i = 1, \dots, m$. Here, logical “OR” is denoted by a “plus” sign. Thus, if $x_j = 1$, it “triggers” two “1”s at the output of the decoder if j is even and a single “1” if j is odd.

The second code C_2 is constructed by an application of the state-splitting algorithm [26]. The modulator of C_2 is fully described by the finite-state machine shown in Fig. 6. At each time instant, the encoder accepts one source bit and outputs two channel bits, the result depending not only on the input but also on the internal state of the machine. To ensure concatenability of all words generated by the modulator, the encoder always starts and finishes in state “A.” This can be achieved by appending a dummy “0” to any input word u . For example, $u = “1110”$ results in $x = “00010010.”$ Thus, all codewords have two extra bits at the end, and the rate of the code is slightly less than $1/2$. If the block length is large, however, this loss in code rate is negligible anyway.

The sliding-window demodulator (SWD) decodes noiseless channel sequences with the help of the decoding table in Fig. 6. Sometimes the decoder can make a decision based on just two input bits. Sometimes, however, it has to look 2 bits ahead; so, in general, the window size is 4 bits. Note that the demodulator makes use of the entire codeword including the last two “dummy” bits generated by the encoder. In reality, of course, the channel output may not obey the $(2, \infty)$ constraint, and the decoder has to deal with “illegal” contents of the sliding window. For simplicity, we output a “1” in this situation, although better decoding strategies are certainly possible.

C. System Comparison Approach

The purpose of this section is to explicitly specify how the benchmark and the constrained systems will be compared against each other. First of all, let $C(a, b)$ stand for the capacity (in bits) of a binary asymmetric channel (BAC) with crossover probabilities a and b . $C(a, b)$ is known to be [27]

$$C(a, b) = \log_2 \left[2^{\frac{aH(b)+(b-1)H(a)}{1-a-b}} + 2^{\frac{bH(a)+(a-1)H(b)}{1-a-b}} \right] \quad (2)$$

where $H(x) = -x \log_2(x) - (1-x) \log_2(1-x)$ is the binary entropy function. Let the benchmark system be characterized by a BAC with crossovers $a_u = p(1|0)$ and $b_u = p(0|1)$. Then, the corresponding channel capacity in bits per second is obviously $C_u = C(a_u, b_u)/T_B$.

The situation after the application of constrained coding is slightly different. The underlying BAC with crossover probabilities a_c and b_c must be estimated at the output of the demodulator before the application of the ECC decoder (Fig. 4).

Let the output of the RLL decoder be an unconstrained binary sequence $v = (v_1, \dots, v_m)$ with possible errors introduced by both the channel and the demodulator itself. Ignoring potential correlations between errors, the crossovers can be estimated as $a_c = p(v_i = 1|u_i = 0)$ and $b_c = p(v_i = 0|u_i = 1)$. Due to the application of a rate $1/2$ RLL code, the channel capacity C_c in bits per second is computed as $C_c = C(a_c, b_c)/2T_B$.

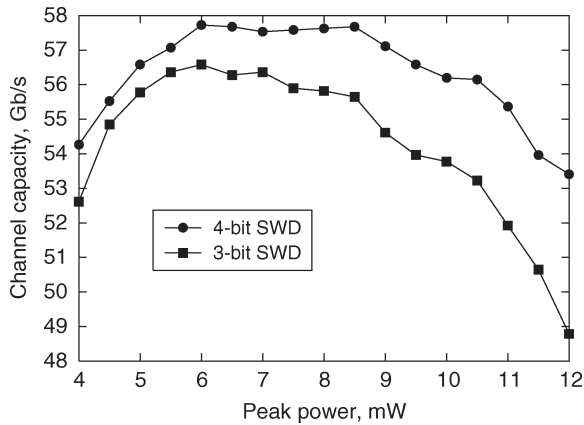
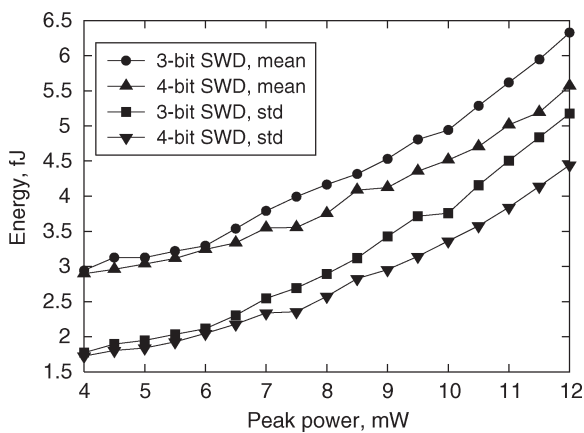
This method of calculating C_u deserves additional comments. First of all, if the crossovers of the BAC are unequal, the capacity-achieving distribution is nonuniform. For example, if $a_u < b_u$, “0”s must occur more frequently than “1”s in the channel bit stream. However, virtually all ECCs used in practice are linear, and “0”s and “1”s are equiprobable at the output of the ECC encoder. Hence, no linear code can achieve the true capacity of a BAC, in principle. Fortunately, it can be shown that the uniform input distribution implies a negligibly small penalty in the achievable data rate. For example, when $p_u = 0.01$, the loss is below 0.07% for all possible pairs of a_u and b_u . Because of this important observation, we do assume that the input distribution is uniform and compute p_u as $(a_u + b_u)/2$. The same discussion is applicable to the constrained system and its probability of error p_c . The latter is obtained as $p_c = (a_c + b_c)/2$.

IV. CONSTRAINED SYSTEM ANALYSIS

It might seem that application of a rate $1/2$ RLL code should “decrease” the capacity C_c of the coded system relative to the capacity C_u of the uncoded system. However, this is not the case. Since every pair of “1”s in the coded system is separated by at least two “0”s, T_B can be reduced by a factor of up to 3 while still preserving at least the same minimum pulse separation Δ and, hence, approximately the same intensity of IFWM-induced perturbations. The pulse shape used in the coded system and the benchmark system can remain identical, thus preserving the transmission bandwidth. If the channel were perfect, the application of a rate $1/2$ RLL code combined with a factor of 3 speedup in effective symbol rate would yield a 50% increase in capacity. This is the key observation of this paper.

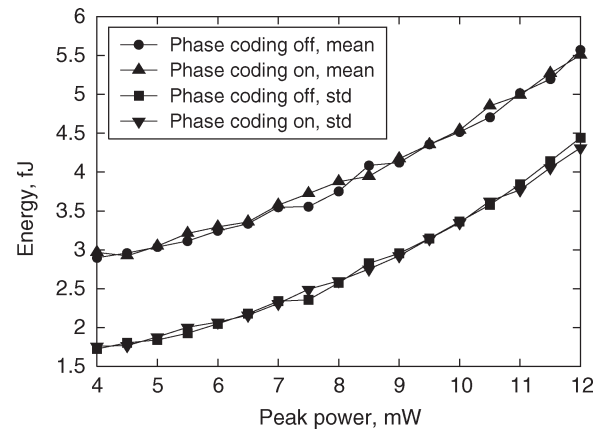
To estimate the potential gain in data rate for a realistic optical channel, we simulated constrained systems with $T_B = 8.35$ ps. Exactly the same pulse shape (with the same pulse parameters) as in the benchmark systems described in Section II was used so that no extra bandwidth was consumed. Again, the peak power P_0 was varied in the range of 4–12 mW. Simulations were carried out using 24 000-bit pseudorandom constrained sequences. A lower bound on the channel capacity was calculated with the help of (2) based on the experimental crossovers a_c and b_c obtained at the output of the RLL decoder. A potential data rate improvement of about 50% for both schemes is clearly visible in Fig. 7. More specifically, the maximum value of C_c was estimated to be 56.6 Gb/s for code C_1 and 57.7 Gb/s for code C_2 . The gain with respect to the benchmark system without phase coding is thus 50.8% and 53.9%. Even when phase coding is applied, the constrained systems still provide an increase of 47.2% and 50.2%, respectively.

Another purpose of the experiment was to compare the performance of RLL codes C_1 and C_2 . A comparison in terms of

Fig. 7. Channel capacity for code C_1 (3-bit SWD) and C_2 (4-bit SWD).Fig. 8. Energy in spaces for code C_1 (3-bit SWD) and C_2 (4-bit SWD).

channel capacity (Fig. 7) favors C_2 , which clearly outperforms its rival throughout the entire range of P_0 . It is also insightful to compare the energy accumulated in “0” bit slots at the receiver for both schemes (Fig. 8). Ideally, it must be close to 0. In a real system, both ASE and IFWM gradually pump energy into spaces so its distribution at the output of the link is far from trivial. Nevertheless, a comparison of means and variances shows consistent advantage of C_2 from the point of view of ghost pulse suppression. At low P_0 , most of the energy in “0”s is due to ASE noise, so the distributions are almost identical. As the contribution of IFWM decreases, the difference becomes more and more clear.

The results obtained may be explained by the fact that the two schemes generate constrained sequences with different distributions of “0”s and “1”s. The first important issue is the probability q_1 that a randomly selected channel bit is a “1.” For code C_2 , $q_1 = 1/6$ (16.67%), while for code C_1 , $q_1 = 5/28$ (17.86%). Mathematically, the lower is the number of “1”s in the transmitted bit stream, the fewer are the interacting doubles and triples they create. Physically, the less energy is pumped into the fiber at the input, the weaker are the nonlinear interactions among the pulses. To validate this conjecture, we designed a third $(2, \infty)$ -constrained code with $q_1 = 5/24$ (20.83%). The performance of that scheme was clearly worse in comparison with either one considered here.

Fig. 9. Energy in spaces with and without phase coding for RLL code C_2 .

The second critical factor is that the introduction of constrained coding makes channel words more irregular. As observed in [10], irregularity helps in ghost pulse suppression since it breaks the resonant nature of intrachannel interactions. Moreover, certain configurations of bits that lead to the formation of strong ghost pulses are now less likely to occur or are entirely forbidden. For example, a benchmark system with no phase coding is known to suffer mostly from sequences like “1110111” or “11011.” The reason is that these sequences contain many pairs and triples of pulses that pump energy into the central “0” via IFWM.

Equivalent $(2, \infty)$ -constrained representations of these “worst” words would be “1001001000001001001” and “1001000001001.” However, the modulator in Fig. 6 never delivers such an output. Indeed, a run of two “0”s (“1001”) can only be produced by a state sequence “BAB,” the leading “1” always occupying an even position in the bit stream. After that, the encoder is always in state “A” and cannot immediately generate another “1.” Therefore, the block “1001001” is forbidden by the encoding machine, and the first worst configuration of bits is eliminated. The second bad sequence begins with a “1001” so the first “1” must be located at even position. However, there is also another “1001” that would start at an odd position in that case. Again, since it is prohibited by the structure of the encoder, the corresponding worst sequence never occurs at the output of the modulator. A quick analysis reveals that code C_1 does not forbid either block, although their probabilities of occurrence are rather low.

We have also simulated constrained systems with additional phase coding and found no significant difference from the systems without phase coding (Fig. 9). This result is actually not surprising. The coding approach in [8] is aimed against the worst channel sequences and suppresses the strongest ghost pulses. Such sequences simply do not occur in our constrained system, i.e., the strongest ghosts have already been busted.

V. MULTICHANNEL EXPERIMENTS

So far, in this paper, we have considered single-channel links, which provide us with considerable physical insight. Modern lightwave systems, however, often transmit information via

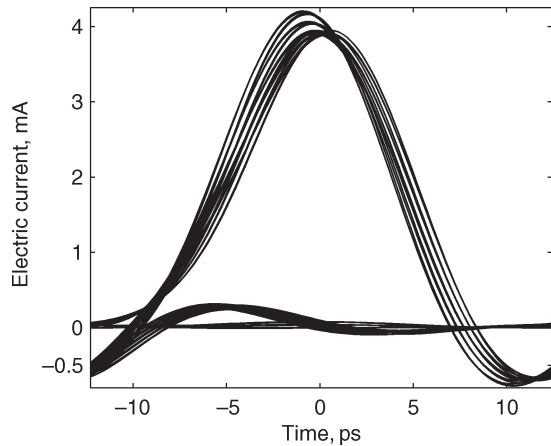


Fig. 10. Back-to-back electrical eye diagram for the second channel of the WDM benchmark system $P_0 = 6$ mW.

several channels simultaneously. Thus, an important practical question is whether constrained coding can be beneficial for WDM systems as well.

Intuitively, the answer must be affirmative since IFWM, an intrachannel phenomenon, is still the dominant impairment in the multichannel case. It is not so obvious, however, as constrained systems operate with shorter bit slots. Hence, they may be more sensitive to interchannel effects. The goal of this section is to demonstrate that the extension of the constrained coding approach to multiple channels is indeed possible, with similar gains as in the single-channel systems.

A. Benchmark WDM System Design

For simplicity, we design a four-channel WDM link based on the benchmark system in Section II. Although the number of channels is usually greater in practice, our setup allows one to capture the impact of interchannel effects while keeping the simulation time reasonable. As in Section II, we also assume no residual dispersion per amplifier spacing and perfect dispersion compensation at the receiver for all channels. Clearly, this picture is a simplification of a real WDM system. Nevertheless, it provides a challenging test for the constrained coding method.

The pulse shape for all channels is given by (1). The carrier frequency of the first channel is 193.25 THz (1552.37 nm), and the channel spacing is set to 180 GHz. Thus, the receiver structure must be modified to reject neighboring channels more efficiently. More specifically, both the optical and the electrical filters are chosen to be fifth-order Butterworth with bandwidths $B_o = 170$ GHz and $B_e = 60$ GHz, respectively. Because of the interchannel crosstalk, the eye diagrams for the first and the fourth (outer) channels are more open than for the second and third (inner) ones. If all channels are initially aligned, the back-to-back electrical eye diagram for the second channel looks like the one in Fig. 10.

Numerical simulations were carried out with almost the same parameters as in Section II, although, perhaps, the number of bits transmitted was insufficient to fully capture interchannel interactions. Essentially, the two inner channels exhibited very similar behavior and so did the outer ones. As expected, it is the

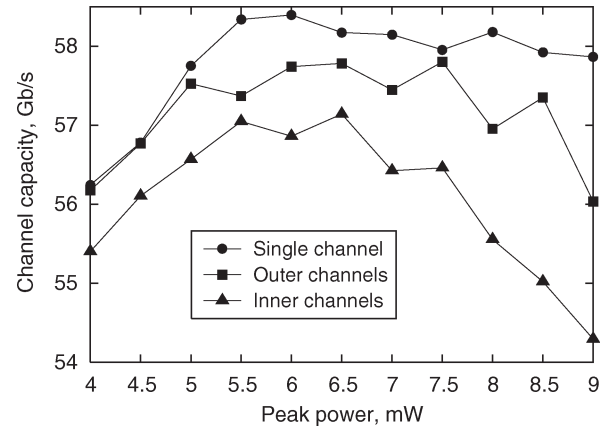


Fig. 11. Four-channel constrained system capacity for inner and outer channels with respect to the single-channel case.

inner channels that limit the system performance. Therefore, we decided to approximate a lower bound on system capacity C_u based on the average probability of error for inner channels observed at the receiver. At $P_0 = 6$ mW, C_u was estimated to be around 38.0 Gb/s. The results did not change significantly when P_0 varied a little. This value of C_u is slightly higher than in the single-channel case thanks to a more advanced receiver structure.

B. Constrained WDM System Results

A four-channel constrained WDM system with channel spacing of 180 GHz is designed in exactly the same manner as in Section IV. Naturally, each channel is encoded independently by an RLL code of interest. In this section, we work with code C_2 only as it proved to be superior to C_1 . The receiver structure is chosen to be the same as for the benchmark WDM system except that the bandwidth of the electrical filter is changed to $B_e = 90$ GHz. Again, we are interested in the average probability of error for both the inner and outer channels, separately.

Fig. 11 shows three different capacity curves of interest obtained from Monte Carlo simulations. As before, the capacity of individual channels was calculated with the help of (2). Again, there exists an optimum region of operation where the probability of error is minimal. Although the results fluctuated quite a bit due to the relatively short bit sequences used, the shape of the curves is in agreement with intuition. As expected, the capacity of the inner channels is noticeably less than that of the outer ones.

The single-channel limit is obtained from the upper curve in Fig. 7 via processing the simulated waveforms by the WDM receiver. As in the benchmark system case, the introduction of a more advanced receiver structure increases the maximum C_c from 57.7 up to 58.4 Gb/s. The most interesting result in Fig. 11 is that the outer channels approach the capacity of the single-channel system when the regime of propagation becomes close to linear. The most important result, however, is that the maximum capacity for the inner channels is 57.1 Gb/s, which still presents a 50.2% increase with respect to the benchmark system.

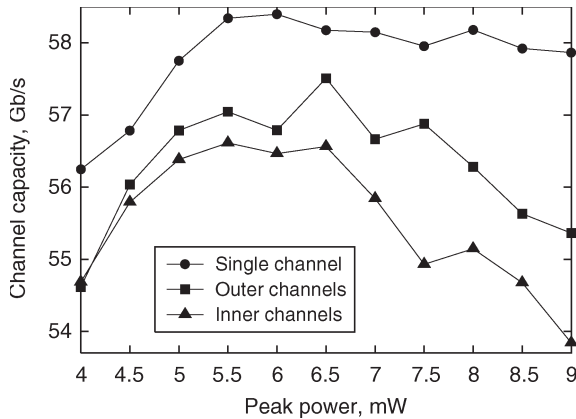


Fig. 12. Eight-channel constrained system capacity for inner and outer channels with respect to the single-channel case.

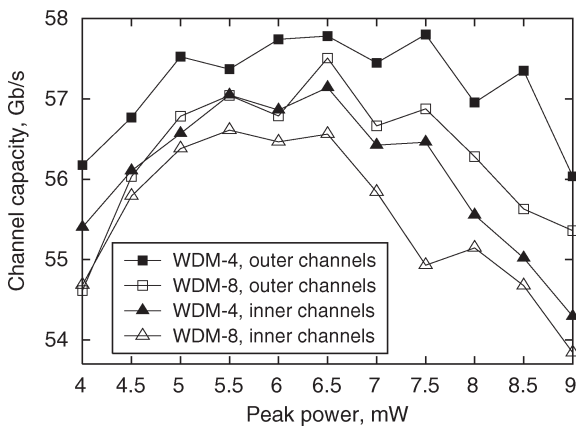


Fig. 13. Constrained systems with four and eight channels are compared against each other.

C. Extension to More Channels

An important question is how the constrained system may be affected by a greater number of channels. In order to address this issue, we added another four channels to the WDM system designed in Section V-B. After that, numerical simulations were carried out for exactly the same set of parameters as in the four-channel case. The results are presented in Fig. 12. The channel capacity declines further, reaching a maximum of about 56.6 Gb/s for the inner channels. Nonetheless, this still corresponds to a 49.0% gain with respect to the benchmark system. For the sake of better illustration, the two constrained WDM systems are compared in Fig. 13. Since the only principal distinction between them is the number of channels, collision-induced timing jitter must be responsible for both the overall jitter growth and the reduction in channel capacity.

VI. DISCUSSION AND CONCLUSION

In this paper, we investigated the application of constrained coding to quasi-linear optical communication systems limited by IFWM. We proposed a particular coding scheme that suppresses the ghost pulses and provides a data rate improvement of up to 50%. The results obtained in our examples indicate that this kind of gain is quite achievable for both single-channel and WDM links. The implementation of a constrained system

requires very little extra hardware since both modulator and demodulator are extremely simple.

Our study assumes an ideal ECC with rate R equal to the channel capacity. For example, if $a_c = b_c = 0.013$, $R = C_c = 0.9$. Certainly, real ECCs always have an extra overhead implying an additional loss in data rate, i.e., $R < C_c$. Nevertheless, this practical issue does not affect our main conclusion. First of all, since p_u and p_c are virtually identical, ECCs with approximately the same redundancy are required in both cases. Furthermore, recent results indicate that designing codes with rates close to capacity is feasible [28]. Hence, our system comparison approach is still fair even when the ECC overhead is taken into account.

It is conceivable that with tighter channel packing, the inter-channel effects may ultimately degrade the probability of error for the constrained system below an acceptable level. In this case, by simultaneously increasing T_B and Δ , the influence of various impairments as well as p_c can be reduced at a certain expense in data rate. Finding the best operating point for such a system involves a number of tradeoffs and presents an interesting topic for future research.

REFERENCES

- [1] A. Mecozzi, C. B. Clausen, and M. Shtaif, "Analysis of intrachannel nonlinear effects in highly dispersed optical pulse transmission," *IEEE Photon. Technol. Lett.*, vol. 12, no. 4, pp. 392–394, Apr. 2000.
- [2] —, "System impact of intra-channel nonlinear effects in highly dispersed optical pulse transmission," *IEEE Photon. Technol. Lett.*, vol. 12, no. 12, pp. 1633–1635, Dec. 2000.
- [3] A. Mecozzi, C. B. Clausen, M. Shtaif, S.-G. Park, and A. H. Gnauck, "Cancellation of timing and amplitude jitter in symmetric links using highly dispersed pulses," *IEEE Photon. Technol. Lett.*, vol. 13, no. 5, pp. 445–447, May 2001.
- [4] P. Johannisson, D. Anderson, A. Berntson, and J. Mårtensson, "Generation and dynamics of ghost pulses in strongly dispersion-managed fiber-optic communication systems," *Opt. Lett.*, vol. 26, no. 16, pp. 1227–1229, Aug. 2001.
- [5] M. J. Ablowitz and T. Hirooka, "Resonant intrachannel pulse interactions in dispersion-managed transmission systems," *IEEE J. Sel. Topics Quantum Electron.*, vol. 8, no. 3, pp. 603–615, May/June 2002.
- [6] J. Zweck and C. R. Menyuk, "Analysis of four-wave mixing between pulses in high-data-rate quasi-linear subchannel-multiplexed systems," *Opt. Lett.*, vol. 27, no. 14, pp. 1235–1237, Jul. 2002.
- [7] R. I. Killely, H. J. Thiele, V. Mikhailov, and P. Bayvel, "Reduction of intrachannel nonlinear distortion in 40-Gb/s-based WDM transmission over standard fiber," *IEEE Photon. Technol. Lett.*, vol. 12, no. 12, pp. 1624–1626, Dec. 2000.
- [8] X. Liu, X. Wei, A. H. Gnauck, C. Xu, and L. K. Wickham, "Suppression of intrachannel four-wave-mixing-induced ghost pulses in high-speed transmission by phase inversion between adjacent marker blocks," *Opt. Lett.*, vol. 27, no. 13, pp. 1177–1179, Jul. 2002.
- [9] N. Alic and Y. Fainman, "Data-dependent phase coding for suppression of ghost pulses in optical fibers," *IEEE Photon. Technol. Lett.*, vol. 16, no. 4, pp. 1212–1214, Apr. 2004.
- [10] S. Kumar, "Intrachannel four-wave mixing in dispersion managed RZ systems," *IEEE Photon. Technol. Lett.*, vol. 13, no. 8, pp. 800–802, Aug. 2001.
- [11] C. Xie, I. Kang, A. H. Gnauck, L. Möller, L. F. Mollenauer, and A. R. Grant, "Suppression of intrachannel nonlinear effects with alternate-polarization formats," *J. Lightw. Technol.*, vol. 22, no. 3, pp. 806–812, Mar. 2004.
- [12] A. Chowdhury, G. Raybon, R.-J. Essiambre, J. H. Sinsky, A. Adamiecki, J. Leuthold, C. R. Doerr, and S. Chandrasekhar, "Compensation of intrachannel nonlinearities in 40 Gb/s pseudo-linear systems using optical phase conjugation," *J. Lightw. Technol.*, vol. 23, no. 1, pp. 172–177, Jan. 2005.
- [13] B. Vasic, V. S. Rao, I. B. Djordjevic, R. K. Kostuk, and I. Gabitov, "Ghost-pulse reduction in 40-Gb/s systems using line coding," *IEEE Photon. Technol. Lett.*, vol. 16, no. 7, pp. 1784–1786, Jul. 2004.

- [14] I. B. Djordjevic and B. Vasic, "Constrained coding techniques for the suppression of intrachannel nonlinear effects in high-speed optical transmission," *J. Lightw. Technol.*, vol. 24, no. 1, pp. 411–419, Jan. 2006.
- [15] I. B. Djordjevic, S. K. Chilappagari, and B. Vasic, "Suppression of intrachannel nonlinear effects using pseudoternary constrained codes," *J. Lightw. Technol.*, vol. 24, no. 2, pp. 769–774, Feb. 2006.
- [16] I. B. Djordjevic, B. Vasic, and V. S. Rao, "Rate 2/3 modulation code for suppression of intrachannel nonlinear effects in high-speed optical transmission," *Proc. Inst. Electr. Eng.—Optoelectronics*, vol. 153, no. 2, pp. 87–92, Apr. 2006.
- [17] N. Kashyap, P. H. Siegel, and A. Vardy, "Coding for the optical channel: The ghost-pulse constraint," *IEEE Trans. Inf. Theory*, vol. 52, no. 1, pp. 64–77, Jan. 2006.
- [18] K. A. S. Immink, *Coding Techniques for Digital Recorders*. London, U.K.: Prentice-Hall, 1991.
- [19] D. Marcuse, "Derivation of analytical expressions for the bit-error probability in lightwave systems with optical amplifiers," *J. Lightw. Technol.*, vol. 8, no. 12, pp. 1816–1823, Dec. 1990.
- [20] P. A. Humblet and M. Azizoglu, "On the bit error rate of lightwave systems with optical amplifiers," *J. Lightw. Technol.*, vol. 9, no. 11, pp. 1576–1582, Nov. 1991.
- [21] O. V. Sinkin, R. Holzlohner, J. Zweck, and C. R. Menyuk, "Optimization of the split-step Fourier method in modeling optical-fiber communication systems," *J. Lightw. Technol.*, vol. 21, no. 1, pp. 61–68, Jan. 2003.
- [22] L. K. Wickham, R.-J. Essiambre, A. H. Gnauck, P. J. Winzer, and A. R. Chraplyvy, "Bit pattern length dependence of intrachannel nonlinearities in pseudolinear transmission," *IEEE Photon. Technol. Lett.*, vol. 16, no. 6, pp. 1591–1593, Jun. 2004.
- [23] V. Pechenkin and F. R. Kschischang, "A new coding scheme for runlength-limited channels," in *Proc. 22nd Biennial Symp. Commun.*, Kingston, ON, Canada, Jun. 2004, pp. 130–132.
- [24] —, "Higher bit rates for dispersion-managed soliton communication systems via constrained coding," *J. Lightw. Technol.*, vol. 24, no. 3, pp. 1149–1158, Mar. 2006.
- [25] G. Khachatrian and K. A. S. Immink, "Construction of simple runlength-limited codes," *Electron. Lett.*, vol. 35, no. 2, p. 140, Jan. 1999.
- [26] K. A. S. Immink, P. H. Siegel, and J. K. Wolf, "Codes for digital recorders," *IEEE Trans. Inf. Theory*, vol. 44, no. 6, pp. 2260–2299, Oct. 1998.
- [27] R. B. Ash, *Information Theory*. New York: Dover, 1990.
- [28] T. Mizouochi, "Recent progress in forward error correction for optical communication systems," *IEICE Trans. Commun.*, vol. E88-B, no. 5, pp. 1934–1946, May 2005.



Vladimir Pechenkin received the B.Sc. and M.Sc. degrees (both with honors) in applied physics and mathematics from the Moscow Institute of Physics and Technology, Moscow, Russia, in 1999 and 2001, respectively. He is currently working toward the Ph.D. degree in electrical engineering at the University of Toronto, Toronto, ON, Canada.

His research interests are mainly in the area of error-control coding, especially for optical communications.

Mr. Pechenkin was the recipient of a number of scholarships (including the Edward S. Rogers Sr. Scholarship) while at the University of Toronto.



Frank R. Kschischang (S'83–M'91–SM'00–F'06) received the B.A.Sc. degree (with honors) from the University of British Columbia, Vancouver, BC, Canada, in 1985, and the M.A.Sc. and Ph.D. degrees from the University of Toronto, Toronto, ON, Canada, in 1988 and 1991, respectively, all in electrical engineering.

He is a Professor of electrical and computer engineering and a Canada Research Chair in communication algorithms with the University of Toronto, where he has been a faculty member since 1991.

During 1997–1998, he spent a sabbatical year as a Visiting Scientist with the Massachusetts Institute of Technology (MIT), Cambridge, and in 2005 was a Guest Professor with the ETH, Zurich, Switzerland. He has taught graduate courses in coding theory, information theory, and data transmission. His research interests are focused on the area of coding techniques, primarily on soft-decision decoding algorithms, trellis structure of codes, codes defined on graphs, and iterative decoders.

Dr. Kschischang was the recipient of the Ontario Premier's Research Excellence Award. From October 1997 to October 2000, he served as the Associate Editor for Coding Theory for the IEEE TRANSACTIONS ON INFORMATION THEORY. He also served as Technical Program Co-Chair for the 2004 IEEE International Symposium on Information Theory held in Chicago, IL.